http://dx.doi.org/10.5012/bkcs.2011.32.10.3707

Preparation and Characterization of Silver Nanoparticles Embedded in Silica Sol Particles

Byung-Kyu Kang, Dong-Min Son, and Youhyuk Kim*

*Department of Chemistry and Institute of Basic Sciences, College of Advanced Sciences, Dankook University, Cheonan, Chungnam 330-714, Korea. *E-mail: hyukim@dankook.ac.kr*
Received July 2, 2011, Accepted August 22, 2011

Silver nanoparticles coated with silica can be obtained by the reduction of $AgNO_3$ with hydrazine in the presence of NaOH-stabilized, active silicic acid (polysilicic acid). The size of the silver nanoparticles and the silica shell thicknesses were affected by varying the hydrazine content, the active silicic acid content and the experimental method (*e.g.* hydrothermal method). Typically, silver nanoparticles sized around 40 nm were aggregated, connected by silica. The presence of peaks centered around 400 nm in UV-vis spectra corresponds to the surface plasmon resonance of silver nanoparticles. The size of the aggregated silver nanoparticles increased with increasing hydrazine concentration. Under hydrothermal conditions at 150 °C the formation of individual silica particles was observed and the sizes of the silver nanoparticles were reduced. The hydrothermal treatment of silver nanoparticles at 180 °C gives a well-defined $Ag@SiO_2$ core-shell in aggregated silica sol particles. The absorption band observed at around 412 nm were red-shifted with respect to the uncoated silver nanoparticles (λ_{max} = 399 nm) due to the larger refractive index of silica compared to that of water. The formation of silver nanoparticles coated with silica is confirmed by UV-visible absorption spectra, transmission electron microscopy (TEM) and energy-dispersive spectroscopy (EDS) data.

Key Words : Silver nanoparticles, Active silicic acid, Hydrothermal method, $Ag@SiO_2$, TEM

Introduction

Research on silver colloids has received a great deal of scientific and economic interest in the past decade because of their applications in surface enhanced Raman spectroscopy (SERS), metal enhanced fluorescence (MEF), catalysis and antimicrobial agents.[1-5] The synthesis of silver colloids is generally performed by the reaction of silver salts with reductive agents and stabilizing agents.[6,7] The silver colloidal suspensions have a tendency of being aggregated by the addition of a ligand or by aging, and this hinders the application of silver colloids for many industrial processes. The embedding of silver nanoparticles in silica matrices has been used for the stabilization of silver nanoparticles and for their fixation and immobilization onto many substrates.[8,9] Among the stabilizing agents previously tested, silica shows distinct advantages over organic stablizing agents: (1) optical transparency, (2) chemical inertness, (3) photochemical stability (4) cheapness, and (5) colloidal stability.[10] In addition to these, silica provides the surface roughness and distance between the silver surface and the adsorbate needed for MEF applications. Direct contact between the adsorbate and the metal surface is reported to be fatal for the emission intensity.[11] In order to apply silver nanoparticles to different surfaces it is most beneficial to have a liquid solution of stabilized silver nanoparticles that could be easily applied by dip-coating or spraying. The method of silica sol preparation in silver colloids extensively reported in the literature involves the Stöber synthesis of colloidal silica with[12] or without[13-15] silane coupling agents as surface primers. These methods require careful experimental conditions, such as optimization of the concentrations of tetraethoxysilane (TEOS), ethanol, water and amine. Although a uniform silica shell is attained with these methods, they comprise more than three steps: the preparation of silver colloids with citrate stabilizer, the generation of siloxy groups on the surface of the nanoparticles using a silane coupling agent, and the addition of silica shell forming agents with basic catalyst. A simple preparation method for Ag/SiO_2 sols would greatly expand the range of potential applications for silver nanoparticles. In industry, the preparation of silica sols involves active silicic acid, which is generated from inexpensive water glass.[16] Here we present the results of a synthesis and characterization of silver nanoparticles embedded in silica sol particles. This method consists of the generation of a silver colloid in active silicic acid (polysilicic acid) by the reduction of $AgNO_3$ with hydrazine in a single step and the hydrothermal treatment of the silver colloid. The use of hydrazine as a reductive agent in the present work is of importance, since this produces high concentrations of silver colloids without undesired side products. The reduction of $Ag^+(aq)$ by $N_2H_4(aq)$ is given as follows:[17,18]

$$4Ag^+(aq) + N_2H_4(aq) + 4OH^-(aq) \rightleftharpoons 4Ag^0(s) + N_2(g) + 4H_2O$$

For some applications, the reagents used in the colloid preparation could produce undesired reactions or spectral interference with the Raman signal of the adsorbate.[19-21]

Experimental

Materials. Sodium silicate (water glass, commercial, 28%), NaOH (Duksan, 96%), $AgNO_3$ (Aldrich, 99+%), $N_2H_4{\cdot}H_2O$ (Aldrich, 98%), and cation-exchange resin (Samyang Co., TRILITE SCR-B) were used.

Synthesis of Active Silicic Acid. Active silicic acid was prepared using the ion-exchange method.[16] The active silicic acid was stabilized by adding NaOH to give an aqueous solution of pH 9-10.

Synthesis of Nanosilver Particles Embedded in Silica Sol Particles. Different volumes (0.014 mL, 0.027 mL, 0.083 mL, 0.135 mL, 0.270 mL) of hydrazine ($N_2H_4{\cdot}H_2O$) was immediately added into 50 ml of an aqueous solution of active silicic acid, while $AgNO_3$ (0.093 g, 0.54 mmol) was prepared separately in 25 mL of distilled water. The silver colloids in the active silicic acid were generated by slowly dropping silver nitrate solution into an active silicic acid solution with hydrazine. The molar ratios of $AgNO_3$ to N_2H_4 ranged from 2 to 1/10. The solution was centrifuged at 14000 rpm/min for 20 min and the sediment washed with alcohol and distilled water several times. The supernatant of silver colloidal sol in active silicic acid was placed in a polytetrafluoroethylene vessel that was then placed inside a stainless steel autoclave with a mechanical stirrer. The autoclave was maintained at 150 °C for 2 h, cooled naturally to 100 °C, and then water-cooled to room temperature.

Characterization. The elemental composition, morphology and sizes of the resulting products were analyzed using a transmission electron microscope (TEM; JEOL JEM-3010) operating at 300 kV and energy-dispersive X-ray spectroscopy (EDS) using an INCA X-Sight spectroscope (Oxford Instruments). The absorption spectra of the silver colloid sols were recorded on a UV2201 Shimadzu UV-VIS spectrophotometer using optical quartz cells.

Results and Discussion

Generation of Silver Nanoparticles in Active Silicic Acid. The silver colloids were synthesized by the chemical reduction of $AgNO_3$ using hydrazine as a reducing agent in the presence of NaOH-stabilized active silicic acid. The color of the solution was reddish brown under all synthesis conditions. To obtain silver nanoparticles with more uniform dimensions, the reaction mixtures were centrifuged. Figure 1 shows the UV-vis spectra for the supernatant of the silver colloid at various molar ratios of $AgNO_3$ over hydrazine. The presence of peaks centered around 400 nm corresponds to the surface plasmon resonance of silver nanoparticles.[12] There also are shoulders at around 420 nm, suggesting some aggregation of silver nanoparticles in low concentrations of hydrazine. With increasing hydrazine concentration, the intensities of the surface plasmon resonances were decreased and the shape of absorption band appeared to be broad. The silver nanoparticles in active silicic acid exhibited the formation of silica shells, regardless of the hydrazine concentration. Figure 2 shows TEM images of the

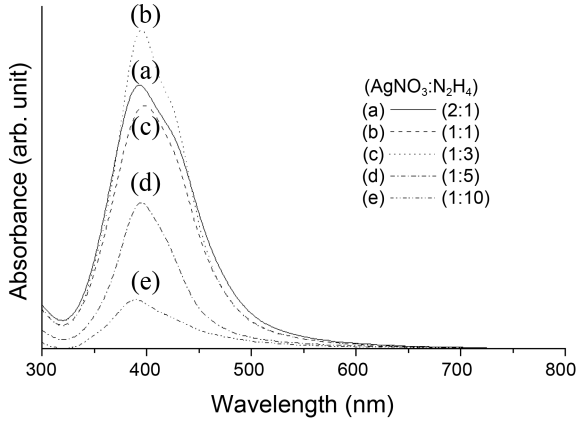

Figure 1. UV-vis spectra of silver colloids with various molar ratios of $AgNO_3$ (7.20×10^{-3} M) to N_2H_4.

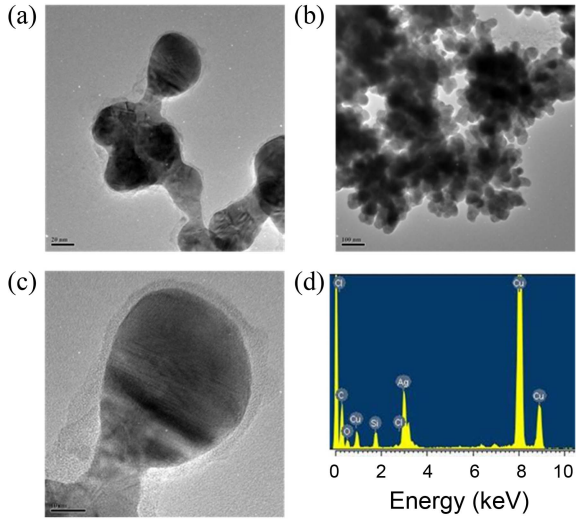

Figure 2. TEM images of (a) the supernatant and (b) the sediment of silver colloids with a 1:1 molar ratio of $AgNO_3$ (7.20×10^{-3} M) to N_2H_4, (c) enlarged picture of (a) showing silica shell formation and (d) EDS spectraum of (c).

supernatant and the sediment of the silver nanoparticles prepared at a molar ratio of hydrazine over $AgNO_3$ = 1 and EDS results confirm that Si, O, and Ag atoms are present. Small spherical silver nanoparticles sized around 40 nm were aggregated by connection with silica and the aggregation was more pronounced among the samples that had sedimented, as expected, as shown in Figure 2(b). The sediment can be characterized by the collection of small silver nanoparticles coated with silica. The silica shell thickness of the final silver nanoparticles in the supernatant is around 3-5 nm, as shown in Figure 2(c). However, formation of individual silica particles was not observed under all experimental conditions. This suggests that polymerization of active silicic acid bound to the metal surfaces occurs easily compared to that of free active silicic acid to give silica sol particles. With increasing hydrazine concentration, the sizes of the silver nanoparticles coated with silica in the sediment increase, as shown in Figure 3. This explains the lower intensities of the surface plasmon bands at higher

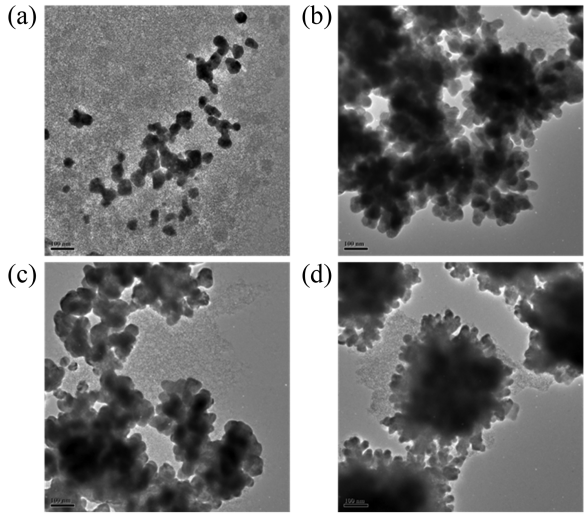

Figure 3. TEM images of the sediment of silver colloids with various molar ratios of $AgNO_3$ (7.20×10^{-3} M) to N_2H_4, (a) 2:1, (b) 1:1, (c) 1:3, (d) 1:10.

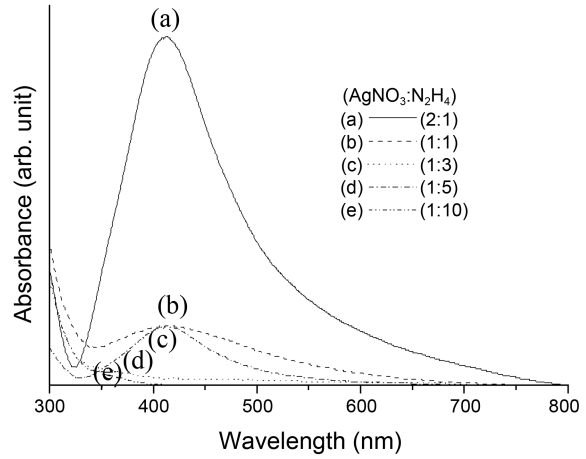

Figure 4. UV-vis spectra of the supernatant of silver colloids with various molar ratios of $AgNO_3$ (7.20×10^{-3} M) to N_2H_4 after hydrothermal treatment.

concentrations of hydrazine in Figure 1.

Hydrothermal Reaction of the Supernatant. The hydrothermal method is a thermal treatment in water at temperatures higher than the boiling point of water, in which an autoclave is necessary to keep the spontaneous pressure. The hydrothermal method is frequently used in industry to grow silica particles from active silicic acid.[16] Figure 4 shows the absorption spectra of hydrothermally treated supernatants. The surface absorption bands observed at around 412 nm were red-shifted with respect to the uncoated silver nanoparticles (λ_{max} = 399 nm) reported in the literature.[22] It is known that the surface plasmon absorption band is very sensitive to both particle size and shape, and to the properties of the surrounding medium.[23-26] The red-shift of the surface plasmon band is due to the larger refractive index of silica compared to that of water. At high hydrazine concentrations, no surface plasmon bands due to silver nanoparticles were observed. These results are understood since initial

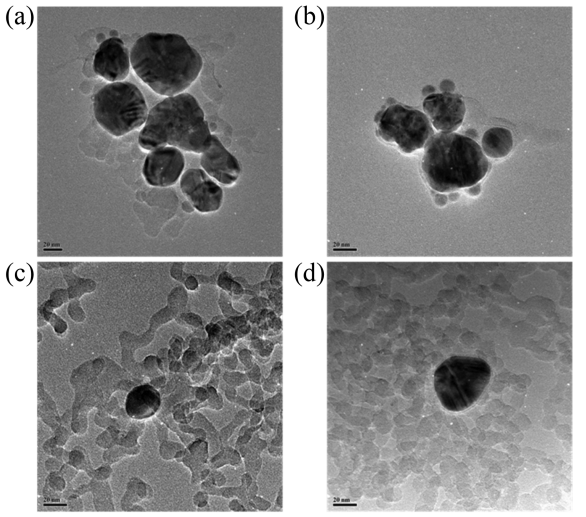

Figure 5. TEM images of the supernatant of silver colloids with various molar ratios of $AgNO_3$ (7.20×10^{-3} M) to N_2H_4, (a) 2:1, (b) 1:1, (c) 1:3, (d) 1:5 after hydrothermal treatment.

concentration of silver nanoparticles in high hydrazine concentrations was so low. Figure 5 shows typical TEM images of hydrothermally treated active silicic acid containing silver nanoparticles in the supernatant prepared using various concentrations of the initial $AgNO_3$ solution. With increasing hydrazine concentrations, the formation of individual silica sol particles was observed and the sizes of silver nanoparticles were reduced. It is interesting to note that the morphology of the silica sol particles changed from round to elongated silica sols, and then to larger round ones as the hydrazine concentration was increased. The size of the silica sol particles increased from around 5 nm to 15 nm with increasing hydrazine concentration, as shown in Figure 5(b) and (d). Since the solubility in water of the silica sol increases with temperature, the crystal growth is accelerated in hydrothermal treatment by a dissolution-recrystallization process. It is known that large crystals such as quartz (α-SiO_2) and anatase or rutile (TiO_2) are obtained by this treatment.[27-29] The reduction and formation of more rounded shapes of the silver nanoparticles is also observed, especially compared to the sediment of silver nanoparticles in Figure 3. These observations might be explained by the dissolution of silver nanoparticles through hydrolysis of water to give silver ions and hydroxide ions under hydrothermal conditions. In this system hydrazine seems to be involved in the process of polymerization of active silic acid. The degree of polymerization increases with increasing hydrazine concentration. The polymerization of active silicic acid occurs at the surface of the silver nanoparticles, as shown in Figure 5(a) and (b). Thus, silica particle polymerization takes place in non-uniform directions, and an elongated silica sol is formed as shown in Figure 5(c). The elongated silica sols have a diameter of about 10 nm and a length of 50-100 nm. It is known that elongated silica sols have better film-forming properties compared with spherical ones, and elongated sols are used as a binder or coating agent for the formation or

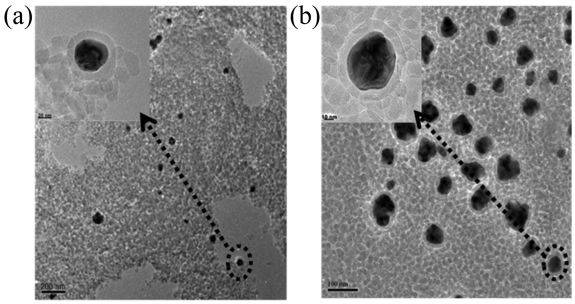

Figure 6. TEM images of hydrothermally treated active silicic acid containing silver colloids with various concentrations of $AgNO_3$: (a) 2.72×10^{-3} M, and (b) 9.06×10^{-3} M. The molar ratio of $AgNO_3$ to N_2H_4 was 1:3.

surface treatment of inorganic fibers. Indeed, the mixture of a calcium salt, an active silicic acid, and an aqueous sodium hydroxide is heated in an autoclave at 100-150 °C for several hours to prepare elongated silica sols.[30]

Ag@SiO_2 Core-Shell Embedded in Silica. To obtain more densely populated silver nanoparticles, several concentrations of $AgNO_3$ in the presence of active silicic acid were reduced by hydrazine and treated under hydrothermal conditions without the process of centrifugation. The autoclave was maintained at 180 °C for 4 h, cooled naturally to 100 °C, and then water-cooled to room temperature. Figure 6 shows typical TEM images of hydrothermally treated active silicic acid containing silver nanoparticles. At such concentrations, the formation of well-defined, dense, Ag@SiO_2 core-shell nanoparticles was observed. Ag@SiO_2 core-shell particles with silver diameters in the range 20-80 nm and a silica shell thickness of about 8-10 nm were embedded in the aggregated silica matrices. The silica particles in the silica matrices were around 20 nm in size. The silica shell thickness was slightly increased to around 10 nm during the hydrothermal reaction under this experimental condition. The elemental composition of the Ag@SiO_2 core-shell particles was analyzed by energy-dispersive spectroscopy, as shown in Figure 6. Si, O and Ag atoms were found as expected. The silver nanoparticle distribution is found to be uniform based on TEM, as shown in Figure 6(a) and (b). Figure 7 shows the absorption spectra of these samples and the surface absorption bands observed at around 420 nm were red-shifted with respect to the silver nanoparticles before hydrothermal treatment. This is consistent with theoretical predictions[15] and TEM results in Figure 6, which correlate the red-shift with an increase in the local dielectric constant surrounding the silver nanoparticles that is due to increasing silica shell thickness. The absorption band of Figure 7(b) shows lower intensity and broader shape compared to that of Figure 7(a). This suggests that the size distribution of silver nanoparticles becomes more polymodal with increasing the concentration of $AgNO_3$.

To separate the Ag@SiO_2 core-shell nanoparticles from the aggregated silica particles, the solution was centrifuged at 8000 rpm/min and the sediment and the supernatant were analyzed by TEM. Complete isolation of the Ag@SiO_2 core-

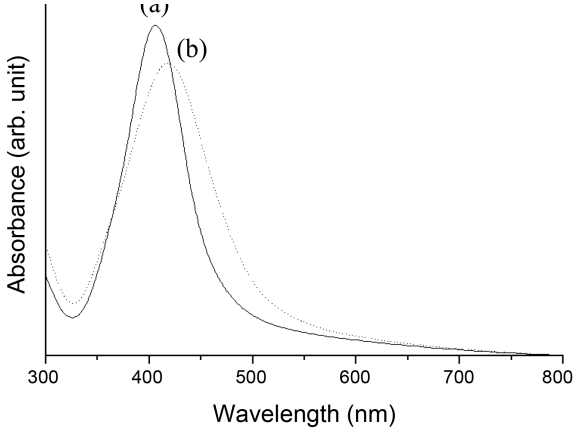

Figure 7. UV-vis spectra of hydrothermally treated active silicic acid containing silver colloids with various concentrations of $AgNO_3$: (a) 2.72×10^{-3} M, and (b) 9.06×10^{-3} M. The molar ratio of $AgNO_3$ to N_2H_4 was 1:3.

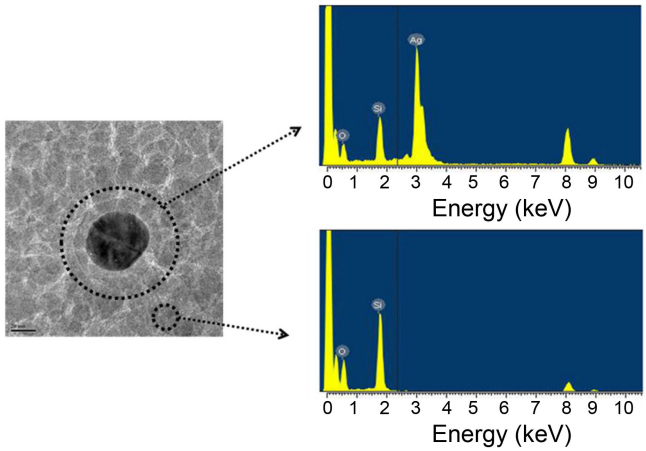

Figure 8. TEM image and EDS spectra of hydrothermally treated active silicic acid containing silver colloids with a concentration of $AgNO_3$ of 7.26×10^{-3} M. The molar ratio of $AgNO_3$ to N_2H_4 was 1:3.

shell particles from the aggregated silica particles could not be achieved, as shown in Figure S1. The concentration of Ag@SiO_2 core-shell particles was larger in the precipitates due to the higher silver density. To investigate the effect of the active silicic acid concentration on the formation of silver particles, several low concentrations of active silicic acid were prepared. At low concentrations, the color of the reaction solutions was black due to the formation of silver precipitates. No surface plasmon band due to silver nanoparticles was observed. The sizes of the silver nanoparticles were reduced after hydrothermal treatment, as observed with a high concentration of active silicic acid. The silver particles exhibited a dendritic morphology, different from that of the silver nanoparticles prepared with high concentrations of active silicic acid (Figure S2).

Conclusions

In order to expand the range of potential applications for silver nanoparticles, a simple preparation method to give a

silica sol solution containing silver nanoparticles has been developed. From the reduction of $AgNO_3$ with hydrazine in the presence of NaOH-stabilized, active silicic acid, silver nanoparticles coated with silica were obtained. The polymerization of active silicic acid bound to the metal surfaces occurs easily compared to that with free active silicic acid to give silica sol particles. The hydrazine, the active silicic acid contents and the experimental method (*e.g.* hydrothermal method) are important in controlling the size of the silver nanoparticles and the silica shell thickness. Under hydrothermal conditions at 150 °C the formation of elongated silica sols was observed. This may be due to the polymerizationin of the active silicic acid in a non-uniform direction at the surface of the silver nanoparticles. The reduction and formation of more rounded silver nanoparticles is also observed. These observations might be explained by a dissolution-recrystallization process in the preparation of the silver nanoparticles. A well-defined $Ag@SiO_2$ core-shell embedded in aggregated silica sol particles can be achieved by using a higher concentration of $AgNO_3$ under the hydrothermal treatment of silver nanoparticles at 180 °C. These preparation methods for coating solutions containing silver nanoparticles would be very useful, not only for the design and fabrication of a number of metal/silica-based nanocomposite materials, but also for temperature-sensitive substrates like textiles or wood.

Acknowledgments. The present research was using a research fund from the Institute of Bio-Science and Technology at Dankook University in 2009.

References

1. (a) Muniz-Miranda, M. *J. Raman Spectrosc*. **2002**, *33*, 295. (b) Halvorson, R. A.; Vikesland, P. J. *Environ. Sci. Technol*. **2010**, *44*, 7749.
2. Li, X.; Zhang, J.; Xu, W.; Jia, H.; Wang, X.; Yang, B.; Zhao, B.; Li, B., Ozaki, Y. *Langmuir* **2003**, *19*, 4285.
3. Gryczynski, I.; Malicka, J.; Shen, Y. B.; Gryczynski, Z.; Lakowicz, J. R. *J. Phys. Chem. B* **2002**, *106*, 2191.
4. Richards, R. *Surface and Nanomolecular Catalysis*; CRC press: Boca Raton, FL, 2006; p 405-407.
5. (a) Mahltig, B.; Gutmann, E.; Reibold, M.; Meyer, D. C.; Böttcher, H. *J. Sol-Gel Sci. Techol.* **2009**, *51*, 204. (b) Sotirioua, G. A.; Teleki, Camenzind, A.; Krumeicha, F.; Meyerb, A.; Pankeb, S.; Pratsinis, S. E. *Chem. Eng. J.* **2011**, *170*, 547.
6. Manikam, V. R.; Cheong, K. Y.; Razak, K. A. *Mater. Sci. Eng. B* **2011**, *176*, 187.
7. Tolaymat, T. M.; El Badawy, A. M.; Genaidy, A.; Scheckel, K. G.; Luxton, T. P.; Suidan, M. *Sci. Tot. Environ*. **2010**, *408*, 999.
8. Kawashita, M.; Tsuneyama, S.; Miyaji, F.; Kokubo, T.; Kozuka, H.; Yamamoto, K. *Biomaterials* **2000**, *21*, 393.
9. Mahltig, B.; Fiedler, D.; BÖttcher, H. *J. Sol-Gel Sci. Techol.* **2004**, *32*, 219.
10. Mulvaney, P.; Liz-Marzan, L. M.; Giersig, M.; Ung, T. *J. Mater. Chem.* **2000**, *10*, 1259.
11. Lakowicz, J. R. *Anal. Biochem*. **2005**, *337*, 171.
12. Liz-Marzan, L. M.; Giersig, M.; Mulvaney, P. *Langmuir* **1996**, *12*, 4329.
13. Yin, Y.; Lu, Y.; Sun, Y.; Xia, Y. *Nano Lett*. **2002**, *2*, 427.
14. Lu, Y.; Yin, Y.; Li, Z.-Y.; Xia, Y. *Nano Lett*. **2002**, *2*, 785.
15. Kobayashi, Y.; Katakami, H.; Mine, E.; Nagao, D.; Konno, M.; Liz-Marzan, L. M. *J. Colloid Interface Sci.* **2005**, *283*, 392.
16. Bergna, H. E.; Roberts, W. O. *Colloidal Silica: Fundamentals and Applications*; CRC press: Boca Raton, FL, 2005; p 47-56.
17. Pourbaix, M. *Atlas of Electrochemical Equlibria in Aqueous Solutions;* National Association of Corrosion Engineers: Houston, TX, 1974; p 393.
18. Cotton, F. A.; Wilkinson, G. Advanced Inorganic Chemistry, 4th ed.; John Wiley and Sons: New York, 1980; p 418.
19. Sbrana, G.; Neto, N.; Muniz-Miranda, M.; Nocentini, M. *J. Phys. Chem.* **1990**, *94*, 3706.
20. Muniz-Miranda, M.; Neto, N.; Sbrana, G. *J. Mol. Struct*. **1988**, *174*, 351.
21. Muniz-Miranda, M. *Colloids Surf. A* **2003**, *217*, 185.
22. Van Hyning, D. L.; Klemperer, W. G.; Zukoski, C. F *Langmuir* **2001**, *17*, 3128.
23. Kobayashi, Y.; Correa-Duarte, M. A.; Liz-Marzan, L. M. *Langmuir* **2001**, *17*, 6375.
24. Moores, A.; Goettmann, F. *New J. Chem*. **2006**, *30*, 1121.
25. Liu, Y.; Liu, C.-Y.; Chen, L.-B.; Zhang, Z.-Y *J. Colloid Interface Sci.* **2003**, *257*, 188.
26. Underwood, S.; Mulvaney, P. *Langmuir* **1994**, *10*, 3427.
27. Matthews, A. *Am. Mineralogist* **1976**, *61*, 419.
28. Oguri, Y.; Riman, R. E.; Bowen, H. K. *J. Mater. Sci*. **1988**, *23*, 2897.
29. Kondo, M.; Shinozaki, K.; Ooki, R.; Mizutani, N. *J. Ceram. Soc. Jpn*. **1994**, *102*, 742.
30. (a) Watanabe, Y.; Ando, *M. European Patent Appl. Publication*; No. A2,0335195, **1989**. (b) Wang, J.; Sugawara, A.; Shimojima, A.; Okubo, T. *Langmuir* **2010**, *26*, 18491.